山口大学教育学部研究論叢　第 75 巻　225 頁～ 233 頁　2026 年 1 月

Visualization of the Particulate and Kinetic Nature of Matter by Utilization of Physical Models, Part IV: Formation of Polymer Secondary Structures

MURAKAMI Kiyofumi（村上清文）, FUJIMURA Taihei（藤村泰平）,
WAIZUMI Kenji（和泉研二）

（Received September 26, 2025）

ABSTRACT

Polymer is one of the major areas covered in upper secondary school chemistry. This paper describes an application of the molecular-movement presentation apparatus, which was constructed to visualize a microscopic molecular motion, to secondary-structure formation by intramolecular interactions and structural changes due to heat in synthetic polymer model and polypeptide model. Spontaneous and reversible helical-structure formation was observed in the synthetic polymer model mimicking poly-isocyanate. However, spontaneous formation of sheet structure was not observed. But, it was found that by introducing a turn structure by fixing the rotation around the bond of the nitrogen atom the sheet structure was formed spontaneously and quickly, showing that the rate-determining step in the formation of the sheet structure is the formation of the turn structure. In the case of the polypeptide model, it was found that 3.0_{10}-helix structure was spontaneously formed among the possible α-helix and 3.0_{10}-helix structures. As in the case of poly-isocyanate model, anti-parallel β-sheet structure was quickly formed in the model in which a β-turn II structure was introduced at the middle of the polypeptide chain, although it could not spontaneously be formed without β-turn II structure. On the other hand, the formation of a repeated β-turn type II structure was also observed, without introducing the β-turn II structure. This structure called silk I has been reported as a precursor structure of silkworm silk before spinning process. These results were discussed from viewpoints of chemical education of synthetic and natural polymers.

1. INTRODUCTION

Understanding the particulate and kinetic properties of matter is essential for promoting students' conceptual understanding of chemical phenomena. However, many assessment studies have revealed that misconceptions about basic properties such as the particulate nature of matter and the spacing between particles (Novick & Nussbaum, 1978, Novick & Nussbaum, 1981, Griffiths & Preston, 1992), the mass of particle (Furio Mas et al., 1987, Stavy, 1988), and the thermal expansion (Novick & Nussbaum, 1981, Griffiths & Preston, 1992, Lin & Lawrenz, 2000), etc. make it difficult for students to achieve conceptual understandings.

Furthermore, these misconceptions make it difficult for students to understand higher-level chemical equilibrium phenomena that build on these conceptual understandings, such as the dynamic nature (Gussarsky & Gorodetsky, 1986, Ozmen, 2008), the reversible feature (Maskill & Cachapuz, 1989, Berquist & Heikkinen, 1990, Ozmen, 2008), the distinction between reaction rate and extent of reaction (Hackling & Garnett, 1985, Banerjee, 1991), the constancy of equilibrium constant (Wheeler & Kass, 1978, Voska & Heikkinen, 2000), and even the application of Le Châtelier's principle (Tyson et al., 1999, Solomonidou & Stavridou, 2001).

In recent years, Murakami et al. (2021a, 2021b) have been trying to develop educational materials that promote conceptual understanding of chemical

Department of Science, Faculty of Education, Yamaguchi University, Yoshida 1677-1, Yamaguchi 753, Japan

phenomena by visualizing particulate and kinetic behavior using physical models of atoms and molecules. They proposed a molecular motion presentation apparatus that can directly measure macroscopic physical quantities such as pressure and volume, while expressing microscopic molecular motion using superballs as physical model molecules. It was clarified that by using this apparatus, it became possible to visualize the microscopic thermal motion of gas molecules, and to show the relationship between macroscopic quantities and microscopic molecular motions, and the relationship between macroscopic quantities expressed by gas law ($PV = nRT$) (Murakami et al., 2021a). Furthermore, as a result of applying the apparatus to chemically interacting systems of a bimolecular binding reaction, it became possible to present the kinetic and reversible nature of chemical equilibrium, the internal energy changes of reaction, the constancy of equilibrium constants, and the approach from a non-equilibrium state to the equilibrium one (Murakami et al., 2021b). These results suggest that the present visualization approach using physical models is helpful in improving above mentioned students' misconceptions about chemical equilibrium, and are leading to further expectation that the present visualization attempts using physical models may also be applied to more complicated chemical reaction systems.

In the previous paper in this series of developing new teaching materials, Murakami et al. (2026) presented van der Waals gas model mimicking water molecules and dimerization and recombination reaction model. In the former case, the characteristic peak behavior of the van der Waals equation of state was observed in an appropriate temperature range and a water-specific cage-like structure (Arata, 1998) was found to be formed under low-temperature conditions. In the latter case, the internal energy change of reaction has been evaluated, and it became possible to draw an activation energy profile of dimerization from the time-dependent data of the reaction.

By further developing new physical model systems, it will be possible to increase the number of situations in which this presentation apparatus can be applied in educational practice. One possible way is to reproduce the process of formation of higher-order structures in polymers. Polymer is one of the major areas covered in high school chemistry. The curriculum guidelines for upper secondary school chemistry (Ministry of Education, 2018) recommend teaching the structure, properties, and composition of typical synthetic fibers and plastics. Furthermore, for natural polymer compounds, it is recommended to treat the structure and properties of proteins, etc. from the perspective of their relationship with monomers. Textbooks describe that polypeptides that make up proteins form α-helix and β-sheet structures due to intramolecular hydrogen bonds (Takeuchi et al., 2021). Regarding protein reactions, heat-induced denaturation is also discussed. However, although textbooks use illustrations to explain these, they are not sufficient to form realistic images of those structure formation and their changes.

If we can demonstrate the dynamic behavior of structure formation due to intramolecular interactions and structural changes due to heat in synthetic polymers and polypeptides using the molecular motion presentation apparatus and a physical model molecule, it is expected that students' conceptual understanding of these phenomena will be promoted. Recently, Bak et al. (2022) have focused on the helix formation and functionalization of poly-isocyanates consisting of successive amide backbone. Because of the narrow spacing between the amide bonds and a strong steric effect between the carbonyl group and the alkyl group, poly-isocyanate has a rigid helical structure. Poly-isocyanates are expected to be used as peptide-mimetic polymers due to their helical structure, functionality, degradability, and high sequence controllability.

In this study, physical models of a hypothetical poly-isocyanate and a polypeptide have been constructed. The possibility of forming secondary structures such as helix structure and sheet structure due to intramolecular hydrogen bonds was examined by using the molecular motion presentation apparatus. This research method could be called physical model simulation. Based on the results, how to use it in chemistry education was discussed.

2. EXPERIMENTAL

2.1 Poly-isocyanate model

As a hypothetical polymer, we constructed a model of poly-isocyanate (Fig. 1), which is the simplest polymer compound with an amide bond as its basic skeleton (Okamoto et al., 1994, Bak et al., 2022). Here, it was assumed that the bond axis between atoms is oriented

toward the vertex of the regular tetrahedron centered on carbon or nitrogen (the amide bond has a planar structure in the ground state, but it is known as an example that the planar structure is broken in the excited state (Oka et al., 2012)). In addition, it was assumed that a hydrogen bond can be formed between an oxygen atom bonded to carbon and a hydrogen atom bonded to nitrogen.

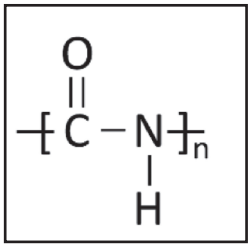

Figure 1. Structure of polyamide.

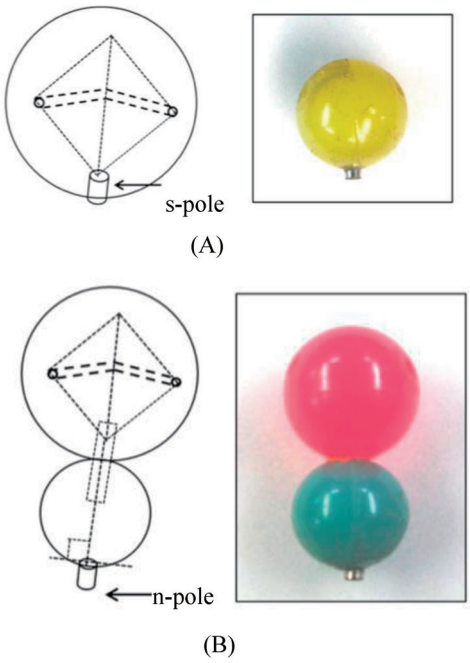

Figure 2. Schematic diagrams and it's physical models of nitrogen atom (A) and carbon and oxygen atoms (B).

Figure 2. shows schematic diagrams and their physical models of nitrogen atom (Fig. 2(A)) and carbon and oxygen atoms (Fig. 2(B)), which construct the present poly-isocyanate model. We used a superball with a diameter of 20 mm and a weight of 3.9 g as the nitrogen atom model, and a cylindrical neodymium magnet with a length of 6 mm and a diameter of 3 mm as the interaction site. Two of the normal directions of the four vertices of the regular tetrahedron inscribed in the superball sphere were drilled with a depth of 10 mm. A hole was drilled into one of the remaining vertices and the cylindrical magnet was embedded so that the south pole protruding 1 mm from the surface. The weight of the superball after embedding the magnet was 4.1g. A 16.5 mm diameter superball was used as the oxygen atom model. A cylindrical magnet of 3 mmΦ×6 mm was embedded in the radial direction of the sphere so that the N pole protruded 1 mm from the surface. A superball with a diameter of 20 mm was used as the carbon atom model, and holes were made in the same way as the nitrogen atom model. The oxygen atom model and the carbon atom model were connected by a bamboo stick and glue. The nitrogen atom model and the carbon atom model, in which the oxygen atom model was bound, were sewn alternately together by using a nylon string, and 22 of them were connected to form the poly-isocyanate model (Fig. 3).

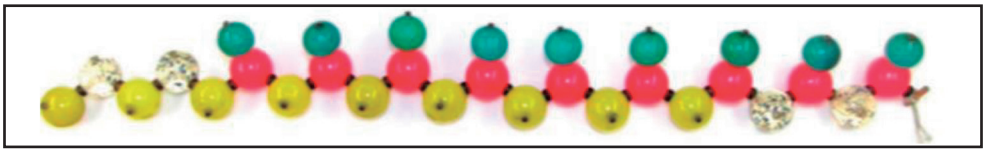

Figure 3. Physical model of poly-isocyanate, in which the nitrogen atom and the carbon atom models are alternatively connected by a string to form polymer.

2.2 Polypeptide model

Considering the bond angles and bond distances of the peptide units (Fig. 4, Hamaguchi, 1976) and the planar structure of the peptide units, the polypeptide model was created with the following specifications (Table 1). The model was created assuming that all the amino acids that constitute the polypeptide model are composed of glycine, i.e. polyglycine. The carbon atom model connected with the side chain was expressed by Cα, and the C=O carbon was expressed by C' to distinguish the carbon atoms. We prepared a nitrogen atom model, a hydrogen atom model, a carbon atom C' model, an oxygen atom model, and a carbon atom Cα model connected with the side chain.

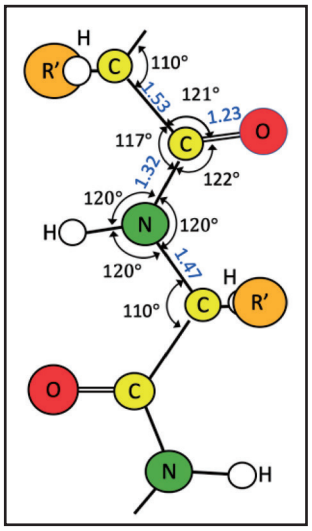

Figure 4. Bond angles and bond distances of the polypeptide units (partially modified from Hamaguchi, 1976)

Table 1. Bond angles of polypeptide and present model.

Atomic array	Bond angle	
	Polypeptide	Present model
CCN	117°	120°
CNC	120°	
CCO	121°	
OCN	122°	
HNC	120°	
NCC	110°	109°

The bond distance between atoms determined so that the bond distance ratios match with those of the real polypeptide, based on the shortest C'-N bond distance. In this model, 16.7 mm diameter superballs are used as atomic models of C' and N, so the bond distance between C' and N was set to 16.7 mm, being the distance between the centers of the two spheres. Furthermore, in order to represent the planar structure of the peptide unit, the C atom and the N atom models were fixed using bamboo sticks to prevent rotation around the C-N axis.

In order to smooth rotation around the rotatable bond axis, cylindrical plastic parts with a diameter of 8 mm with good slippage were embedded in the mutually contacting surfaces of the two atomic models, and the two atomic models came into contact through these parts. These cylindrical plastic parts were covered with a transparent plastic ring with an inner diameter of 8 mm to prevent them from shifting against each other (Fig. 5). Furthermore, the relative lengths between C' and N atoms in the atomic arrangement of C'=O...H-N including hydrogen bond was set to be 50.6 mm so that the relative lengths of the present model match with those of actual polypeptides.

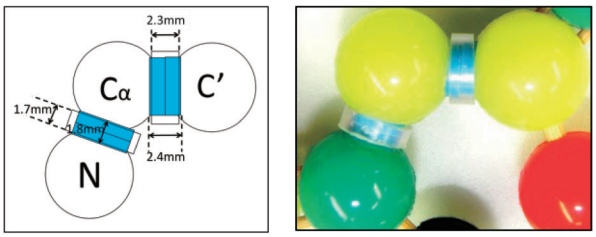

Figure 5. Parts that smooth rotation around the bond axis between atoms. The blue parts are the cylindrical plastic parts with good slippage, and the transparent plastic ring is the parts to prevent the blue plastic parts from shifting against each other (see text).

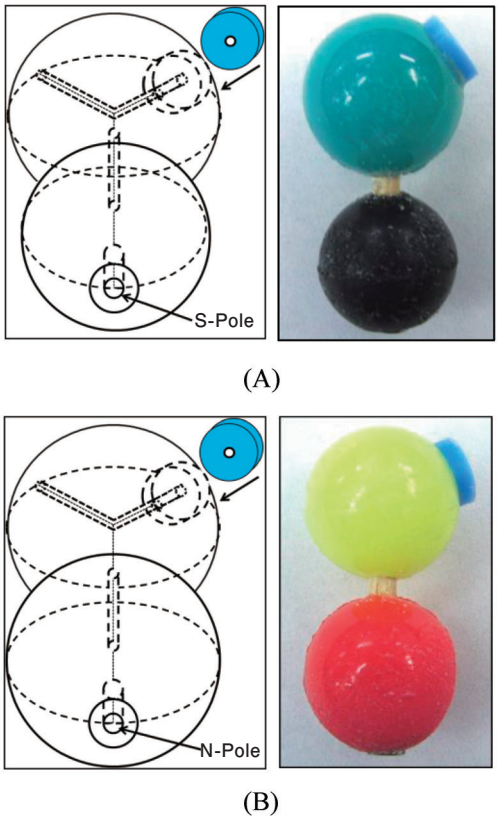

Figure 6. Schematic diagram and physical model of nitrogen-hydrogen model (A) and C' carbon-oxygen model (B) (see text in detail).

2.2.1 Creation of nitrogen-hydrogen model (Fig. 6(A)).

As a model of hydrogen atom, a tip part of a black super ball with a diameter of 14.7 mm was cut flat, and a hole was made on it so that the S pole face of a buried magnet with a diameter of 4 mm x 4 mm was in the same position as the cut surface. For the nitrogen atom model, a 16.7 mm diameter green superball was drilled from three directions so that the bond angles became

120° . At the tip of a hole in one of the three directions, a hole with a diameter of 8 mm, which is the same as the diameter of the blue plastic part, was made on the surface that connects to the Cα atom model, and the plastic part was embedded so that it protruded 2.9 mm from the surface. Another one hole was used to create a bond with hydrogen. This hole was connected using a bamboo stick and an adhesive to another hole drilled on the hydrogen atom model from the opposite position to that in which the magnet was embedded.

2.2.2 Creation of C' Carbon-oxygen model (Fig. 6(B)).

As an oxygen atom model, a tip part of a red superball with a diameter of 16.7 mm was cut flat and then a hole similar to that of the hydrogen atom model was made and the same magnet was embedded so that the N-pole facing outward. A yellow superball with a diameter of 16.7 mm was used as the C' carbon atom model, and holes similar to those of the nitrogen atom model were made. An oxygen atom model was connected to this C' carbon atom model in the same way as the nitrogen-hydrogen atom model, and the blue plastic part was attached to the position where it would bond to the Cα carbon atom so that it protruded 3.2 mm from the surface.

2.2.3 Creation of Cα carbon atom model (Fig. 7).

As the Cα carbon atom model, we used a 16.7 mm diameter yellow superball as well as the C' carbon atom model. Holes with a depth of 9 mm were drilled in two of the normal directions of the four vertices of the regular tetrahedron inscribed in the superball sphere.

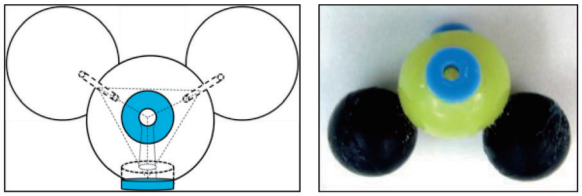

Figure 7. Schematic diagram and physical model of Cα carbon atom model (see text).

The blue plastic parts were attached to these holes so that one plastic part protruded 3.2 mm from the surface that bonded to the nitrogen atom model, and the other plastic part protruded 2.9 mm from the surface that bonded to the C' carbon atom model. Hydrogen atom models of black superballs with a 14.7-mm diameter were attached to the remaining two vertices, as the side chains.

2.2.4 Creation of polypeptide model.

The nitrogen-hydrogen model, the Cα carbon atom model, and the C' Carbon-oxygen model were sewn together by using a nylon string in this order repeatedly through the holes that were made, and 32 pieces of them (ten amino-acid residues) were connected to form a polypeptide model (Fig. 8). By placing the polypeptide model in the molecular motion presentation apparatus and subjecting it to thermal motion, the dynamic behavior of structural changes in the model was observed. The behavior of the model was photographed using a digital video camera recorder (SONY DCR-DVD403).

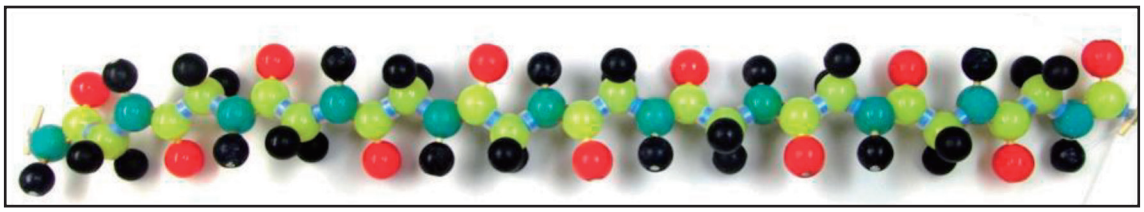

Figure 8. Actual photograph of the created physical polypeptide model (see text).

3. RESULTS and DISCUSSION

3.1 Structure formation of the poly-isocyanate model

It was found that the poly-isocyanate model can form a helical structure (Fig. 9(A)) and a sheet structure (Fig. 9(B)) by hand operation. In the helical structure, seven atoms formed one revolution of the helix. And this helical structure contained nine hydrogen bonds formed by the interaction between S- and N- poles of neodymium magnets. The sheet structure can also be formed when the poly-isocyanate model chain has a turn structure in the middle position. The sheet structure was formed by five hydrogen bonds.

This poly-isocyanate model was put into the molecular motion presentation apparatus, thermal motion was excited, and change in structure was observed. At high temperatures, it was in a random coil state with all

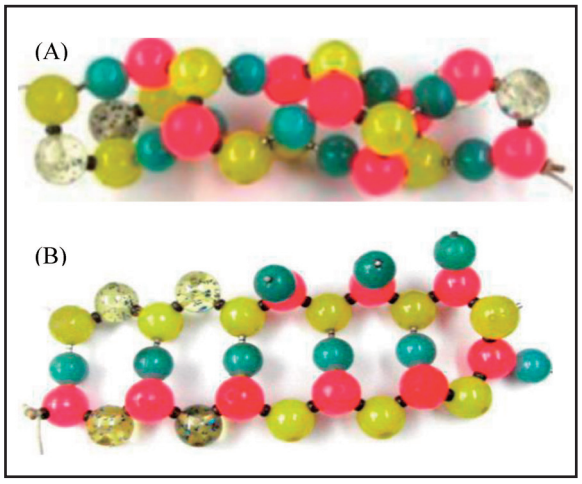

Figure 9. Helical structure (A) and sheet structure (B) formed from the poly-isocyanate model.

hydrogen bonds broken, but as the temperature was gradually lowered, the helical structure of Fig. 9(A) was spontaneously formed as the most stable structure. However, the most stable structure was not formed in every trial, but more unstable structures with different hydrogen bond positions were often formed. It was also observed that the formation of the entire helical structure occurred quickly when two or three hydrogen bonds were formed at the correct positions.

On the other hand, the sheet structure of Fig. 9(B) was not observed to form spontaneously. However, it was found that by introducing a turn structure by fixing the rotation around the bond of the nitrogen atom model with a bamboo stick with a diameter of 2 mm at the position where the poly-isocyanate chain is bisected, the sheet structure was formed spontaneously and quickly. Therefore, it was found that the rate-determining step in the formation of the sheet structure is the formation of the turn structure.

3.2 Structure formation of the polypeptide model

3.2.1 Possible secondary structure.

Polypeptides can form two types of characteristic secondary structures, i.e., helical structures (α-helix structure and 3.0_{10}-helix structure), and β-sheet structures (parallel β-sheet structure and anti-parallel β-sheet structure). In addition to these, there are random structures that have no characteristic regular structure. These structures are characterized by the rotation angle Φ around the N-Cα axis and the rotation angle ψ around the Cα-C' axis (Table 2, Kendrew et al., 1970).

Table 2. Rotation angles of regular structures of polypeptide chain.

Structure	Φ / degree	Ψ / degree
extended chain	+180	+180
α-helix	− 57	− 47
3.0_{10}-helix	− 49	− 26
anti-parallel β-sheet	−139	+135

α-helix structure is also called a 3.6-residue helix because it makes one turn every 3.6 amino acid residues and forms a helical structure with a pitch of 5.4Å. Hydrogen bonds almost parallel to the helical axis are formed between -NH- and -CO- of every fourth amino acid. The amino acid side chains protrude outward from the helix.

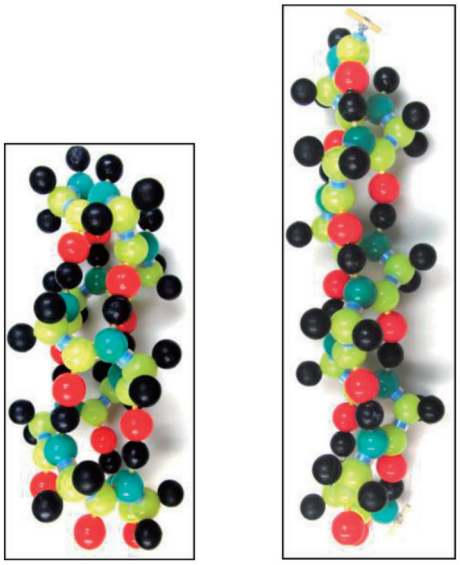

Figure 10. Physical models of α-helix structure (A) and 3.0_{10}-helix structure (B).

3.0_{10}-helix structure has hydrogen bonds between peptides every third residue and is so named because the ring formed by adjacent hydrogen bonds consists of 10 atoms. The constructed physical models of α-helix structure and 3.0_{10}-helix structure are shown in Figure 10. When the polypeptide model chain was bent in the middle of it by introducing the β-turn II structure (Fig. 11(A)), which was made by fixing the rotation around the axes of the C-C and N-C bonds adjacent to the C-N bond, it can form an anti-parallel β-sheet structure (Fig. 11(C)). The sheet structure is formed by five hydrogen bonds.

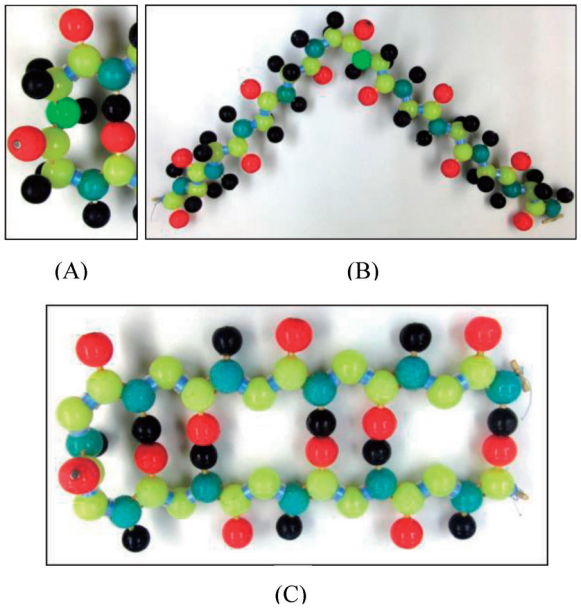

Figure 11. Physical models of β-turn II structure (A) and the random coil form of the model polypeptide in which the β-turn II structure was introduced in the middle (B), and anti-parallel β-sheet structure formed by five hydrogen bonds (C).

3.2.2 Spontaneously formed secondary structures.

The model polypeptide was put in the molecular movement presentation apparatus, and temperature was raised and then cooled slowly.

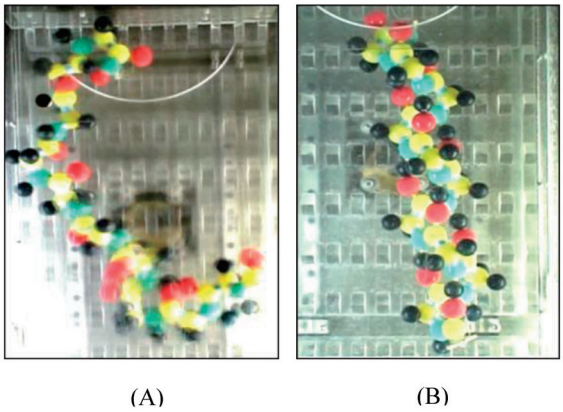

Figure 12. Random coil state (A) at a high temperature, in which all the hydrogen bonds are broken, and 3.010-helix structure formed by slow cooling.

It was found from this procedure that 3.0_{10}-helix structure was spontaneously formed. Figure 12 shows the random coil state at a high temperature, in which all the hydrogen bonds are broken, and the 3.0_{10}-helix structure formed spontaneously by slow cooling. However, the formation of this helical structure did not occur unidirectionally and automatically; the formation and collapse of incorrect hydrogen bonds was repeated over and over until finally two or three correct hydrogen bonds were formed. When this occurred, the formation of the 3.0_{10}-helix structure throughout the entire structure occurred rapidly. No spontaneous formation of α-helix or β-sheet structures could be observed. Improta et al. (2001) have studied the conformation of the infinite polypeptides of glycine, alanine, and α-aminoisobutyric acid in vacuo by quantum mechanical calculations. They obtained α-helix for polyalanine and polyglycine, and 3.0_{10}-helix for poly-α-aminoisobutyric acid as the most stable conformers. On the other hand, Bykov and Asher (2010) concluded from Raman studies that long polyglycine adopts 3.0_{10}-helix structure in aqueous solution. It is interesting to find that the physical model simulation reproduced the secondary structure present in the real polyglycine, even though it was based on simplified parameters (Table 1).

On the other hand, it was confirmed that anti-parallel β-sheet structure was quickly formed in the model in which a β-turn II structure was introduced at the middle of the polypeptide chain. This indicates that, as in the case of poly-isocyanate, the formation of the β-turn structure is the rate-determining process for the formation of the β-sheet structure.

3.2.3 Characteristic secondary structure observed in the polypeptide model.

The structure shown in Figure 13 was also generated by the physical model simulation of the polypeptide model and is called a "repeated β-turn type II structure" (Asakura et al., 2001; Asakura, 2003).

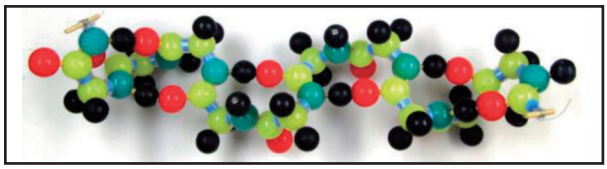

Figure 13. Repeated β-turn type II structure observed in the present physical model simulation.

This structure has been reported as a precursor structure of silkworm silk before spinning process, called silk I. They discovered the repeated β-turn type II structure for a synthesized alanine-glycine alternating co-polypeptides, $(Ala\text{-}Gly)_{15}$. The formation of the characteristic intra-molecular hydrogen bonds along the chain can be seen in Fig. 13. The common feature between the polypeptide they used and the polypeptide

model used in this study is that side chains have small size and are not bulky.

3.3 Educational meaning of the results

From the perspective of teaching the structure and properties of synthetic and natural polymers, the results of the present research are noteworthy for the following points. The first point concerns the reality of states of motion as real substances. Currently, we can use three types of teaching materials for the formation of secondary structures in polymers: the two-dimensional pictorial structural drawings, the creating structures by manually assembling molecular models, and the imaging polymer structures and their changes through computer simulation. However, all of these methods lack the reality and/or dynamism of the structure of real substances. In contrast, the combination of the present polymer models and the thermal motion excitation device enable students to observe the realistic and dynamic behavior of molecular motion, such as rotation around bond axis by thermal excitation and the resulting local structural changes.

Secondly, spontaneous helical-structure formation was realized in both the synthetic poly-isocyanate and polypeptide models, by introducing an elementary hydrogen bond model between oxygen and nitrogen atoms using a magnet. The formation of the helical structure was found to be reversible against temperature change. That is, when the temperature rose above a certain point, the helical structure was broken, and when the temperature dropped below that point, the overall helical structure was reformed after repeated trial-and-error local structural changes in many segments. It is also interesting that the formation of two or three adjacent correct hydrogen bonds was found to be the rate-determining step for the formation of the entire helix structure. Students can observe the detailed process of these structural changes as realistic movements using physical models, and the experience of discovering the rate-determining step from these observations is believed to be valuable in chemistry education.

Third, anti-parallel β-sheet structures were quickly formed in the model polymers by introducing turn structures at the middle of the polymer chain, showing that the rate-determining step in the formation of the sheet structure is the formation of the turn structure. In the case of the present model peptide, fixing two of the 20 rotatable bond axes significantly limits the conformation of the entire peptide chain, leading to the β-sheet structure. This will make students aware of the role and importance of the turn structure in forming sheet structures.

Finally, the discovery of the repeated β-turn type II structure (silk I) by the present physical model simulation, characteristic of alternating alanine-glycine co-polypeptides, is interesting from the perspective of new structural-exploration education using physical models. It may become possible to observe many kinds of structure-formation processes of model molecules having intramolecular or intermolecular interactions in which hydrogen bonds play a major role.

REFERENCES

Arata Y (1998) Book of Water, Kyoritsu Publishing (in Japanese).

Asakura T, Ashida J, Yamane T, Kameda T, Nakazawa Y, Ohgo K, Komatsu K (2001) A repeated b-turn structure in Poly(Ala-Gly) as a model for silk I of bombyx mori silk fibroin studied with two-dimensional spin-diffusion NMR under off magic angle spinning and rotational echo double resonance. *J Mol Biol* **306**, 291-305.

Asakura T (2003) Structure of silks determined with solid-state NMR and development of new silk-like materials. Biophysics **43**, 281-286 (in Japanese).

Bak IG, Chae C-G, Lee, J-S (2022) Synthetic control of helical polyisocyanates by living anionic polymerization toward peptide mimicry. *Macromolecule*s **55**, 1923-1945.

Banerjee AC (1991) Misconceptions of students and teachers in chemical equilibrium. *Int J Sci Educ* **13**, 487-494.

Berquist W, Heikkinen H (1990) Student ideas regarding chemical equilibrium. *J Chem Educ* **67**, 1000-1003.

Bykov S, Asher S (2010) Raman studies of solution polyglycine conformations. *J Phys Chem B* **114**, 6636-6641.

Furio Mas CJ, Perez JH, Harris HH (1987) Parallels between adolescents' conception of gases and the history of chemistry. *J Chem Educ* **64**, 616-618.

Griffiths AK, Preston KR (1992) Grade-12 students' misconceptions relating to fundamental characteristics

of atoms and molecules. *J Res Sci Teach* **29**, 611-628.

Gussarsky M, Gorodetsky E (1986) Misconceptualization of the chemical equilibrium concept as revealed by different evaluation methods. *Eur J Sci Educ* **8**, 427-441.

Hackling MW, Garnett PJ (1985) Misconceptions of chemical equilibrium. *Eur J Sci Educ* **7**, 205-214.

Hamaguchi K (1976) Tanpakushitsu kino no bunshiron, University of Tokyo Press, Tokyo (in Japanese)

Improta R, Barone V, Kudin KN, Scuseria GE (2001) Structure and conformational behavior of biopolymers by density functional calculations employing periodic boundary conditions. I. The case of polyglycine, polyalanine, and poly-α-aminoisobutyric acid in vacuo. *J Am Chem Soc* **123**, 3311-3322.

Kendrew JC, Klyne W, Lifson S, Miyazawa T, Némethy G, Phillips DC, Ramachandran GN, Scheraga H (1970) IUPAC-IUB Commission on biochemical nomenclature: Abbreviations and symbols for the description of the conformation of polypeptide chains. *J. Mol. Biol.* **52**, 1-17.

Lin H-S, Cheng H-J, Lawrenz F (2000) The assessment of students and teachers' understanding of gas laws. *J Chem Educ* **77**, 235-238.

Maskill R, Cachapuz AF (1989) Learning about the chemistry topic of equilibrium: The use of word association tests to detect developing conceptualizations. *Int J Sci Educ* **11**, 57- 69.

Ministry of Education, Culture, Sports, Science and Technology (2018) High school curriculum guidelines commentary, Science section, Notification No. 68, July 2018 (Partially revised in August 2021) https://www.mext.go.jp/content/20211102-mxt_kyoiku02-100002620_06.pdf

Murakami K, Sugimoto T, Waizumi K (2021a) Visualization of the particulate and kinetic nature of matter by utilization of physical models, Part I: Gas laws. *Aust J Ed Chem* **78**, 1-8.

Murakami K, Komatsu Y, Waizumi K (2021b) Visualization of the particulate and kinetic nature of matter by utilization of physical models, Part II: Chemical equilibrium. *Aust J Ed Chem* **78**, 9-15.

Murakami K, Komatsu Y, Fujimura T, Waizumi K (2026) Visualization of the particulate and kinetic nature of matter by utilization of physical models, Part III: van der Waals gas and dimerization and recombination reactions. *Bull Fac Edu Yamaguchi Univ* **75**, 213-223.

Novick S, Nussbaum J (1978) Junior high school pupils' understanding of the particulate nature of matter: An interview study. *Sci Educ* **62**, 273-281.

Novick S, Nussbaum J (1981) Pupils' understanding of the particulate nature of matter: A cross-age study. *Sci Educ* **65**, 187-196.

Oka Y, Morozumi T, Nakamura H (2012) Progress of the fluorescent chemosensor based on the control of twisted intramolecular charge transfer, *Bunseki Kagaku* **61**, 145-156.

Okamoto Y, Matsuda M, Nakano T, Yashima E (1994) Asymmetric polymerization of isocyanates with optically active anionic initiators, *J Poly Sci: PartA: Poly Chem* **32**, 309-315.

Ozmen H (2008) Determination of students' alternative conceptions about chemical equilibrium: A review of research and the case of Turkey. *Chem. Educ Res Pract* **9**, 225-233.

Solomonidou C, Stavridou H (2001) Design and development of a computer learning environment on the basis of students' initial conceptions and learning difficulties about chemical equilibrium. *Educ Inf Tech* **6**, 5-27.

Stavy R (1988) Children's conception of gas. *Int J Sci Educ* **10**, 553-560.

Takeuchi Y et al. (2021) Revised Chemistry (Textbooks of chemistry approved by the Ministry of Education), Tokyo Shoseki (in Japanese).

Tyson L, Treagust DF, Bucat RB (1999) The complexity of teaching and learning chemical equilibrium. *J Chem Educ* **76**, 554-558.

Voska KW, Heikkinen HW (2000) Identification and analysis of student conceptions used to solve chemical equilibrium problems. *J Res Sci Teach* **37**, 160-176.

Wheeler AE, Kass H (1978) Student misconceptions in chemical equilibrium. *Sci Educ* **62**, 223-232.